

See discussions, stats, and author profiles for this publication at: <https://www.researchgate.net/publication/231660650>

# Shape Effects in Molecular Liquids: Phase Equilibria of Binary Mixtures Involving Cyclic Molecules

ARTICLE *in* THE JOURNAL OF PHYSICAL CHEMISTRY B · DECEMBER 1997

Impact Factor: 3.3 · DOI: 10.1021/jp9726551

---

CITATIONS

6

---

READS

13

4 AUTHORS, INCLUDING:



**Eduardo J. M. Filipe**

Technical University of Lisbon

55 PUBLICATIONS 977 CITATIONS

SEE PROFILE



**Jorge C G Calado**

University of Lisbon

115 PUBLICATIONS 1,533 CITATIONS

SEE PROFILE

# Shape Effects in Molecular Liquids: Phase Equilibria of Binary Mixtures Involving Cyclic Molecules

Eduardo J. M. Filipe,\* Luís A. M. Pereira, Lino M. B. Dias, and Jorge C. G. Calado

Complexo I, Instituto Superior Técnico, 1096 Lisboa, Portugal

Richard P. Sear and George Jackson

Department of Chemistry, University of Sheffield, Sheffield, S3 7HF, U.K.

Received: August 13, 1997; In Final Form: October 17, 1997<sup>®</sup>

Using the statistical association fluid theory—hard spheres (SAFT-HS) equation of state for chain molecules and its recent extension to ring molecules, phase diagrams for model mixtures of types ( $m_1$ -sphere chain +  $m_2$ -sphere chain) and ( $m_1$ -sphere chain +  $m_2$ -sphere ring) have been calculated. The influence of chain length, relative sphere size, relative mean-field attraction, and reduced temperature has been investigated. In a first ever application of the SAFT-HS model to cyclic molecules, the theoretical predictions have been compared with experimental data for a variety of systems involving both chain and cyclic molecules. The experimental results confirm the predictions of the theory for the effect of a cyclic molecular structure on the phase behavior of binary mixtures.

## Introduction

Liquid mixtures involving cyclic molecules have been extensively investigated. Almost all possible combinations have been considered: cyclic molecules + linear molecules; cyclic molecules + cyclic molecules; different chain length for both the cyclic and the linear component; both nonpolar (homocycle) and polar (heterocycles) cycles, etc. As a rule, these studies have been restricted to molecules of chain length equal to or greater than five carbon atoms, which are liquid under normal conditions. Most of these molecules can exist in more than one conformation, a circumstance which greatly complicates the discussion of shape effects on the thermodynamic behavior of those mixtures.

In small cyclic molecules (rings of less than five carbon atoms), the absence of internal rotational degrees of freedom makes them rigid and almost free of conformational changes. These molecules are, therefore, more suitable for the discussion of shape effects. They are also, in a structural sense, model molecules and, as such, can usually be well described by simple intermolecular potentials.

As part of a project to assess the role of molecular shape on the thermodynamic behavior of liquid mixtures, we have undertaken a detailed investigation of the excess properties of binary mixtures involving small cyclic molecules. Phase equilibria and density studies of the systems (xenon + cyclopropane),<sup>1</sup> (xenon + cyclobutane),<sup>2</sup> and (xenon + ethylene oxide)<sup>3</sup> as well as those containing their noncyclic analogues, (xenon + propane),<sup>4</sup> (xenon + butane),<sup>5</sup> and (xenon + dimethyl ether)<sup>6</sup> have been carried out (Figure 1). These systems display a wide variety of behavior, from a slightly negative molar excess Gibbs energy,  $G_m^E$ , to liquid–liquid immiscibility. The experimental results show that the mixture containing the cyclic component always exhibits larger positive deviations from Raoult's law (and, consequently, larger values of  $G_m^E$ ) than those occurring with their noncyclic analogues. This effect, however, cannot be exclusively ascribed to a change in molecular shape, since there is a simultaneous modification of

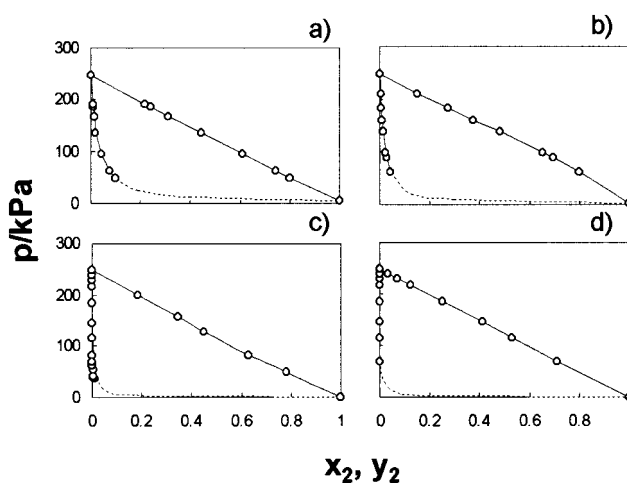


**Figure 1.** Phase diagrams of (a) (xenon + propane);<sup>4</sup> (b) (xenon + cyclopropane);<sup>1</sup> (c) (xenon + butane);<sup>5</sup> and (d) (xenon + cyclobutane)<sup>2</sup> at 182.33 K. The lines are interpolation of the experimental results.

other structural features; namely, (i) the cyclic molecule has two fewer hydrogen atoms; (ii) in small cyclic molecules, the distortion of the bond angles causes a large strain which pushes the electronic density out of the ring, probably interfering with the hydrogen atoms. In cyclic molecules, free rotations around the C–C bonds are hindered, and therefore the hydrogen atoms lie in an almost eclipsed conformation. Consequently, the interaction energy between groups is likely to be different from the corresponding one in a noncyclic molecule. Attempts to separate those different contributions and quantitatively assess the effect of each individual factor are all but impossible to make.

Recently Jackson and co-workers extended their statistical association fluid theory—hard spheres (SAFT-HS) to ring molecules.<sup>7</sup> Using the new theory, we have calculated constant temperature slices of the phase diagram for model mixtures of the ( $m_1$ -sphere chain +  $m_2$ -sphere ring) type and compared the results obtained with those for the corresponding mixtures of chain molecules, ( $m_1$ -sphere chain +  $m_2$ -sphere chain).

<sup>®</sup> Abstract published in *Advance ACS Abstracts*, December 1, 1997.

With this approach we should gain some direct evidence of the effect of substituting, in a binary mixture, a cyclic molecule for an equivalent linear one (same number of spheres). The advantage of using a molecular model of hard spheres for both linear chains and rings is that such a model can only deal with shape; all other structural factors—inevitable when dealing with real molecules—are ignored. In this approach the theoretical predictions are, therefore, a direct consequence of changes in molecular shape alone.

In the present calculations, the influence of chain length, relative sphere size, relative mean-field attraction, and reduced temperature has been investigated.

## Models and Theory

Before we discuss the results of the determination of phase equilibria with the SAFT-HS approach it is convenient to summarize the main expressions of the theory. For further details the reader should consult ref 8 for this version of the theory and ref 9 for the original SAFT approach.

In the SAFT-HS approach, chain and ringlike molecules are described using a simple united-atom model:  $m$  hard-sphere segments of equal diameter  $\sigma$  are bonded tangentially to form a chain or a ring. To examine fluid-phase equilibria in such models, attractive interactions must also be included. We describe the attractive interactions at the van der Waals mean-field level with an integrated interaction energy of  $a$  associated with each segment.

We will give the general equations for mixtures of associating chain and ringlike molecules formed from hard spherical segments with van der Waals interactions and then provide the specific equations for the ( $m_1$ -sphere chain +  $m_2$ -sphere chain) and ( $m_1$ -sphere chain +  $m_2$ -sphere ring) models of interest.

The Helmholtz free energy  $A$  for an  $n$ -component mixture of associating chain or ringlike molecules can be separated into various contributions as

$$\frac{A}{NkT} = \frac{A^{\text{ideal}}}{NkT} + \frac{A^{\text{hs}}}{NkT} + \frac{A^{\text{chain/ring}}}{NkT} + \frac{A^{\text{assoc}}}{NkT} + \frac{A^{\text{mf}}}{NkT} \quad (1)$$

where  $N$  is the total number of molecules,  $T$  is the temperature, and  $k$  is the Boltzmann constant. The ideal contribution to the free energy is given by<sup>10</sup>

$$\begin{aligned} \frac{A^{\text{ideal}}}{NkT} &= \left( \sum_{i=1}^n x_i \ln \rho_i \Lambda_i^3 \right) - 1 \\ &= x_1 \ln \rho_1 \Lambda_1^3 + x_2 \ln \rho_2 \Lambda_2^3 - 1 \end{aligned} \quad (2)$$

The sum is over all species  $i$  of the mixture,  $x_i = N_i/N$  is the mole fraction,  $\rho_i = N_i/V$  the number density,  $N_i$  the number of molecules,  $\Lambda_i$  the thermal de Broglie wavelength of species  $i$ , and  $V$  the volume of the system. The expression of Boublík<sup>11</sup> (equivalent to that of Mansoori et al.<sup>12</sup>) for a multicomponent mixture of hard spheres is used for the reference hard sphere contribution, i.e.,

$$\frac{A^{\text{hs}}}{NkT} = \frac{6}{\pi\rho} \left[ \left( \frac{\xi_2^3}{\xi_3^2} - \xi_0 \right) \ln(1 - \xi_3) + \frac{3\xi_1\xi_2}{(1 - \xi_3)} + \frac{\xi_2^3}{\xi_3(1 - \xi_3)^2} \right] \quad (3)$$

where  $\rho = N/V$  is the total number density of the mixture and the reduced densities  $\xi_i$  are defined as

$$\begin{aligned} \xi_1 &= \frac{\pi\rho}{6} \left[ \sum_{i=1}^n x_i m_i (\sigma_i)^3 \right] \\ &= \frac{\pi\rho}{6} [x_1 m_1 (\sigma_1)^3 + x_2 m_2 (\sigma_2)^3] \end{aligned} \quad (4)$$

$\xi_3 = \eta$  is the overall packing fraction of the mixture, and  $m_i$  is the number and  $\sigma_i$  the diameter of spherical segments of chain or ring  $i$ . The monomer hard-sphere contribution is not the only hard-core repulsive contribution to the free energy, as we must also take into account the effect of forming the hard-sphere chains,<sup>13</sup>

$$\frac{A^{\text{chain}}}{NkT} = - \sum_{i=1}^{n_{\text{chain}}} x_i (m_i - 1) \ln g^{\text{hs}}(\sigma_i) \quad (5)$$

and rings,<sup>7</sup>

$$\frac{A^{\text{ring}}}{NkT} = - \sum_{j=1}^{n_{\text{ring}}} x_j (m_j) \ln g^{\text{hs}}(\sigma_j) \quad (6)$$

Note that the basic difference between the two equations is that in the case of a chain molecule  $m-1$  contacts are counted, whereas in the case of a ring an extra contact is added (the number of contacts equals the number of spheres,  $m$ ).

In general, the contact value of the pair radial distribution function for the spherical segments of species  $i$  and  $j$  in the reference hard-sphere mixture is given by the appropriate Boublík<sup>11</sup> expression as

$$\begin{aligned} g^{\text{hs}}(\sigma_{ij}) &= \frac{1}{(1 - \xi_3)} + 3 \frac{\sigma_i \sigma_j}{\sigma_i + \sigma_j} \frac{\xi_2}{(1 - \xi_3)^2} + \\ &\quad 2 \left( \frac{\sigma_i \sigma_j}{\sigma_i + \sigma_j} \right)^2 \frac{\xi_2^2}{(1 - \xi_3)^3} \end{aligned} \quad (7)$$

The contribution due to association in this case is zero,

$$\frac{A^{\text{assoc}}}{NkT} = 0 \quad (8)$$

Finally, the contribution due to the dispersive attractive interactions is given at the mean-field level in terms of the van der Waals one-fluid theory of mixing:

$$\frac{A^{\text{mf}}}{NkT} = - \frac{\rho}{kT} \sum_{i=1}^n \sum_{j=1}^n a_{ij} x_i x_j m_i m_j \quad (9)$$

In this approach we have expressed the mean-field contribution in terms of segment–segment and not molecule–molecule interactions; that is,  $a_{ij}$  represent the integrated strength of the mean-field attraction per segment.

All the other thermodynamic properties can be obtained from the Helmholtz free energy using the standard relationships. For example, the gas–liquid critical lines can be determined by equating the second and third derivatives of the Gibbs free energy with respect to the mole fraction to zero; phase equilibria between phases I and II require that the temperature, pressure, and chemical potential of each component in each phase are equal, i.e.,

$$T^{\text{I}} = T^{\text{II}}, \quad p^{\text{I}} = p^{\text{II}}, \quad \mu_i^{\text{I}} = \mu_i^{\text{II}} \quad (10)$$

These conditions for phase equilibria are solved numerically

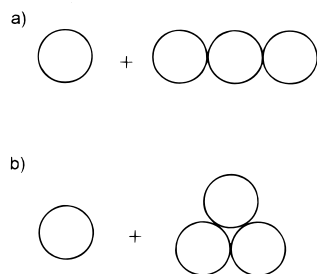


**Figure 2.** Illustration of (a) (1-sphere + 3-sphere ring) and (b) (1-sphere + 3-sphere chain) model mixtures.

using a simplex method. A more detailed description of the techniques is given in ref 14.

As already mentioned, component 1 was kept a chain in all the calculations. For component 2, several chain/ring lengths were used. The sphere diameter ratio,  $\sigma_{22}/\sigma_{11}$ , was changed, as well as the attraction parameter ratio,  $a_{22}/a_{11}$ . The unlike interaction parameters,  $\sigma_{12}$  and  $a_{12}$ , were calculated using the Lorentz–Berthelot rules,

$$a_{12} = (a_{11}a_{22})^{1/2}, \quad \sigma_{12} = (\sigma_{11} + \sigma_{22})/2 \quad (11)$$

## Results and Discussion

The model just described was used to calculate constant temperature slices on phase diagrams for model mixtures of the ( $m_1$ -sphere chain +  $m_2$ -sphere ring) and ( $m_1$ -sphere chain +  $m_2$ -sphere chain) types. For example, the phase diagram of a mixture of a (1-sphere + 3-spheres chain) was calculated and compared with the phase diagram of a mixture of a (1-sphere + 3-spheres ring). Figure 2 illustrates what has just been explained.

The effect of substituting a cyclic molecule for a linear one in a mixture can be assessed comparing the liquidus lines in the liquid–vapor diagram for both cases. As stated before, mixtures containing a cyclic component exhibit larger positive deviations from Raoult's law than those observed for the corresponding noncyclic (linear) case. The main purpose of this work is to check whether the theory can reproduce this type of behavior.

In an earlier work<sup>15</sup> it has been shown that, for the present model, the number of carbon atoms  $C$  in an alkyl chain is related to the number of spherical segments,  $m$ , by the following empirical equation.

$$m = 1 + (C - 1)/3 \quad (12)$$

A value of  $m = 1.33$  will, thus, correspond to ethane,  $m = 1.67$  to propane,  $m = 2$  to butane, etc. This relation is consistent with the fact that, in an  $n$ -alkane, the carbon–carbon bond length is about one-third of the diameter of the cross section of the alkane molecule. In a previous work<sup>4</sup> it was also shown that the xenon atom can be well described by a single sphere,  $m = 1$ , with the same diameter,  $\sigma$ , and attractive parameter,  $a$ , as those of the alkanes (Table 1).

**A. (1-Sphere +  $m_2$ -Sphere Ring) and (1-Sphere +  $m_2$ -Sphere Chain).** The results for model mixtures of types (1-sphere +  $m_2$ -sphere ring) and (1-sphere +  $m_2$ -sphere chain) are shown in Figure 3. In this series of calculations component 1 was kept a sphere, whereas the length (number of spheres) of component 2 varied from  $m_2 = 1.67$  (propane) to  $m_2 = 2, 3$ , and 4. (It should be noted that a ring of less than three spheres can be viewed as a ring of overlapping spheres.) In all cases  $a_{11} = a_{12} = a_{22}$ ,  $\sigma_{11} = \sigma_{22}$ , and  $T_r = T/T_{c1} = 0.7$ .

In all four cases the mixture containing the cyclic component shows more positive deviations from Raoult's law than those

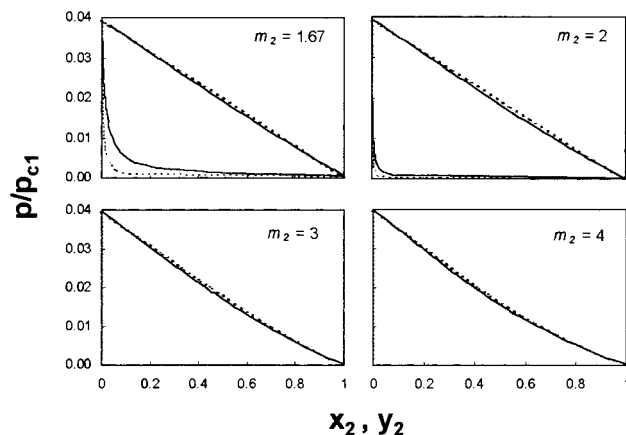


**Figure 3.** Phase diagrams for model mixtures of types (---) (1-sphere +  $m_2$ -sphere ring); (—) (1-sphere +  $m_2$ -sphere chain) at  $T_r = 0.7$ . In all cases  $m_1 = 1$ ,  $a_{11} = a_{12} = a_{22}$ , and  $\sigma_{11} = \sigma_{22}$ .

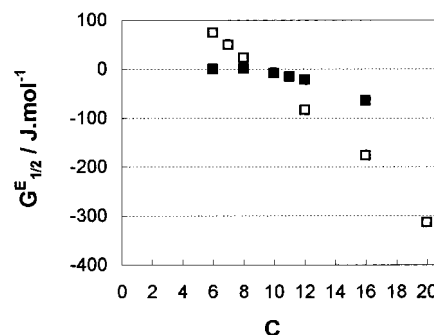


**Figure 4.** Excess molar Gibbs energy for equimolar mixtures of ( $n$ -hexane +  $n$ -alkane) (■) and ( $c$ -hexane +  $n$ -alkane) (□) at 298.15 K, as a function of the number of carbon atoms in the  $n$ -alkane molecule.

**TABLE 1: SAFT-HS Parameters for the Lower  $n$ -Alkanes and Xenon**

molecule	$m$	$\epsilon/k$ (K)	$\sigma$ (Å)
methane	1.00	2109	3.65
ethane	1.33	2890	3.71
propane	1.67	3048	3.85
butane	2.00	3164	3.82
pentane	2.33	3194	3.90
hexane	2.67	3236	3.87
octane	3.33	3236	3.88
xenon	1.00	3198	3.92

exhibited by the chain-containing analogue. This effect becomes less pronounced as the length of component 2 increases: for  $m = 2$  the mixture with the cyclic component shows positive deviations from Raoult's law and for  $m = 1.67$  it is practically ideal, whereas the mixtures with the corresponding noncyclic molecules show, in both cases, negative deviations. These trends are confirmed by the experimental results for the real systems analogues, namely the (xenon +  $n$ -alkane) mixtures, with  $n = 3$ –4 (Figure 1).

**B. ( $m_1$ -Sphere Chain + 2.67-Sphere Chain) and ( $m_1$ -Sphere Chain + 2.67-Sphere Ring).** Liquid mixtures with cyclohexane are, by far, the most investigated systems involving cyclic molecules. In terms of the SAFT-HS theory, the  $n$ -hexane molecule is modeled by  $m = 2.67$ . Experimental studies of mixtures of cyclohexane with almost all  $n$ -alkanes from  $C_5$  to  $C_{16}$  (and also with some cycloalkanes) can be found in the literature.<sup>16–19</sup> The thermodynamic behavior of these mixtures is summarized in Figure 4, where the values of  $G_m^E$  for the equimolar mixture are plotted as a function of the number of carbon atoms in the  $n$ -alkane. (Cyclohexane +  $n$ -alkane) mixtures show  $G_m^E$  values that monotonously decrease with  $n$ ,

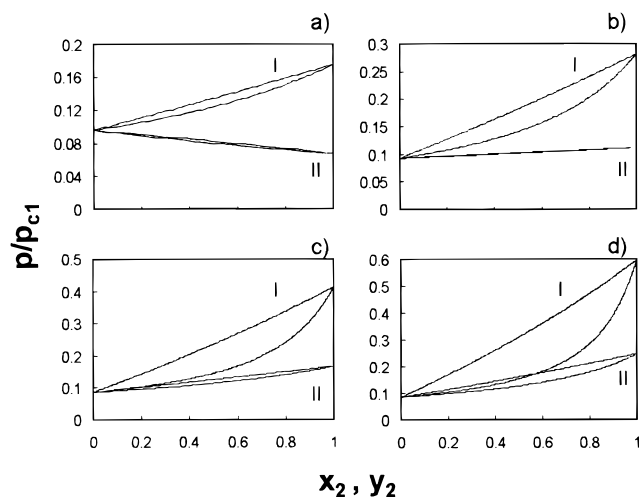


**Figure 5.** Phase diagrams for model mixtures of types ( $m_1$ -sphere + 2.67-sphere chain) (I) and ( $m_1$ -sphere + 2.67-sphere ring) (II) at  $T_r = 0.7$ . (a)  $m_1 = 3.00$ ; (b)  $m_1 = 3.33$ ; (c)  $m_1 = 3.67$ ; (d)  $m_1 = 4.00$ . In all cases  $m_2 = 2.67$ ,  $a_{11} = a_{12} = a_{22}$ , and  $\sigma_{11} = \sigma_{22}$ .

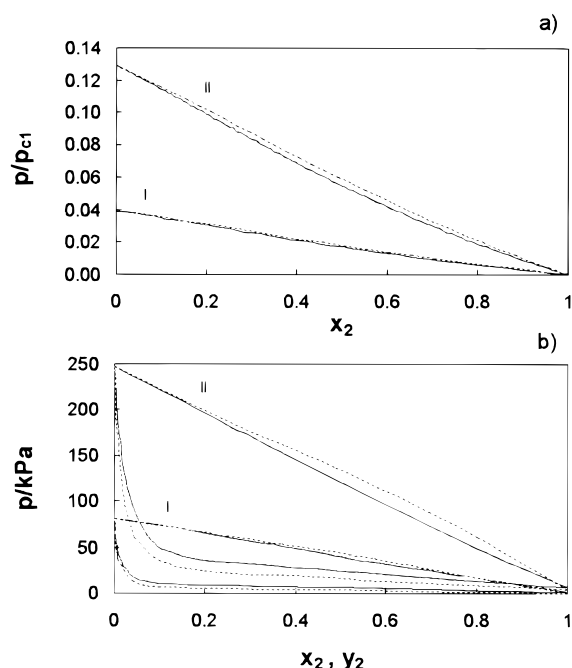


**Figure 6.** (a) Phase diagrams of model mixtures of types (---) (1-sphere + 3-sphere ring); (—) (1-sphere + 3-sphere chain) at (I)  $T_r = 0.6$  and (II)  $T_r = 0.7$ . In both cases  $a_{11} = a_{12} = a_{22}$ , and  $\sigma_{11} = \sigma_{22}$ . (b) Phase diagrams of (---) (xenon + propane);<sup>4</sup> (—) (xenon + cyclopropane)<sup>1</sup> at (I) 161.39 K and (II) 182.33 K.

becoming negative from nonane onward. The corresponding mixtures with *n*-hexane (as opposed to cyclohexane) follow a similar trend, but are practically ideal up to octane, only exhibiting small negative  $G_m^E$  values from nonane onward.<sup>20–23</sup> This complex behavior is related to both the ordering of the liquid *n*-alkanes, as their chain length increases, and the fact that cyclohexane, being a globular molecule, acts as a “structure breaker” when mixed with *n*-alkanes.

Phase diagrams for model mixtures of types ( $m_1$ -sphere chain + 2.67-sphere chain) and ( $m_1$ -sphere chain + 2.67-sphere ring) were calculated and are shown in Figure 5. The chain length (number of spheres) of component 1 took the values  $m_1 = 3.00$ , 3.33, 3.67, and 4.00, corresponding to *n*-heptane, *n*-octane, *n*-nonane, and *n*-decane. As before,  $a_{11} = a_{12} = a_{22}$ ,  $\sigma_{11} = \sigma_{22}$ , and  $T_r = 0.7$  in all cases.

As can be seen, the theory predicts that the mixtures

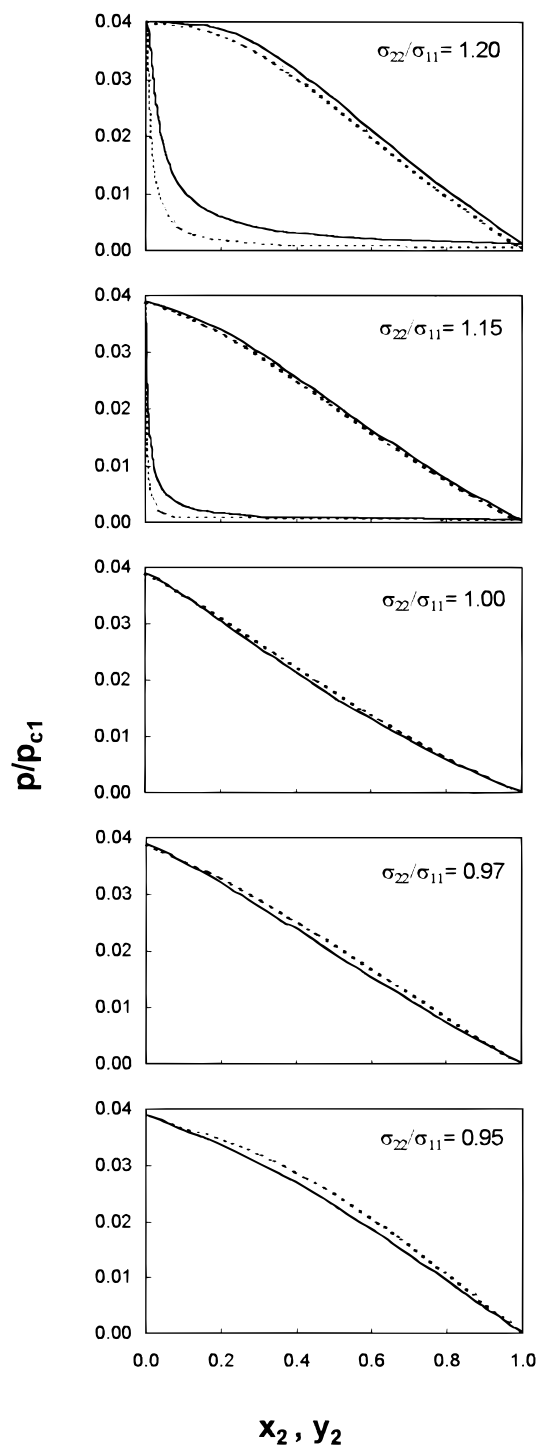


**Figure 7.** Phase diagrams for model mixtures of types (---) (1-sphere + 3-sphere ring); (—) (1-sphere + 3-sphere chain) at  $T_r = 0.7$  and different  $\sigma_{22}/\sigma_{11}$  ratios. In all cases  $m_1 = 1$ ,  $m_2 = 3$ , and  $a_{11} = a_{12} = a_{22}$ .

containing the cyclic component should show more positive deviations from Raoult's law than the corresponding values for mixtures with the linear component. This is confirmed by the experimental behavior of the (*n*-heptane + cyclohexane) and (*n*-octane + cyclohexane) mixtures only. The theory is not able to predict the crossover observed in Figure 4. It is interesting to note, however, that the theory predicts positive deviations from Raoult's law for mixtures of cyclohexane with heptane or octane, but negative deviations from Raoult's law for mixtures of cyclohexane with nonane or decane, in agreement with the experimental results.

### C. Temperature, Relative Sphere Size, and Mean-Field

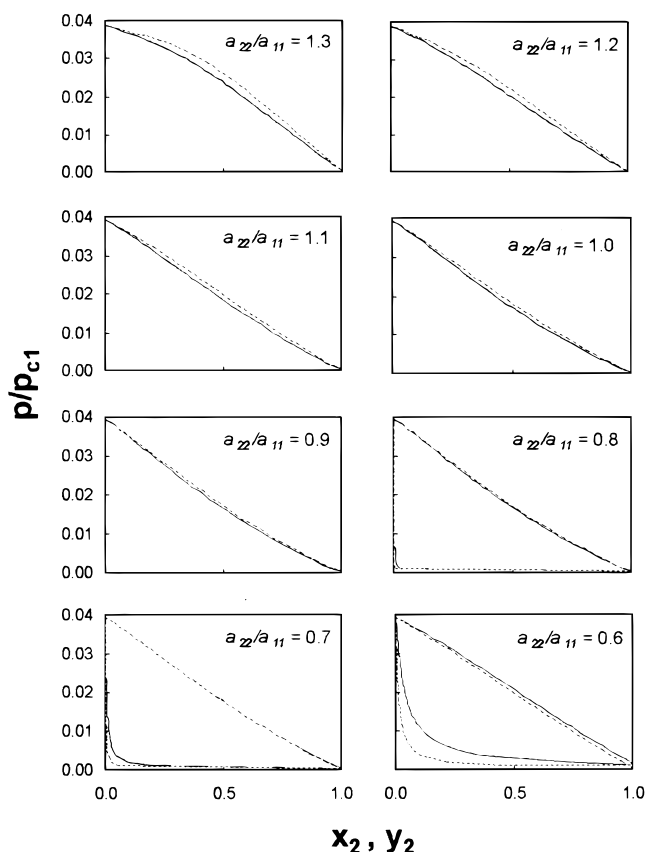


**Figure 8.** Phase diagrams for model mixtures of types (---) (1-sphere + 3-sphere ring); (—) (1-sphere + 3-sphere chain) at  $T_r = 0.7$  and different  $a_{22}/a_{11}$  ratios. In all cases  $m_1 = 1$ ,  $m_2 = 3$ , and  $\sigma_{11} = \sigma_{22}$ .

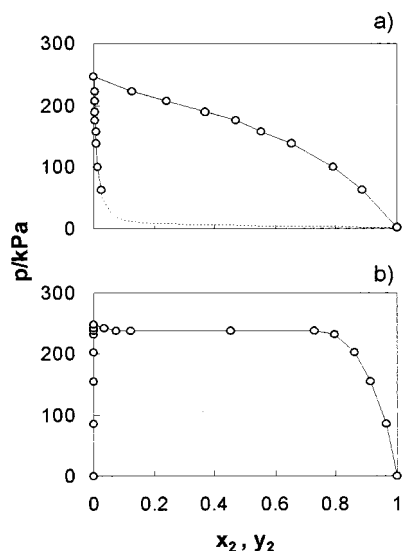


**Figure 9.** Phase diagrams of (a) (xenon + dimethyl ether);<sup>6</sup> (b) (xenon + ethylene oxide)<sup>3</sup> at 182.33 K. The lines are interpolation of the experimental results.

**Attraction Parameter Effects.** The effects of temperature, relative sphere size, and mean-field attraction on the liquid–vapor phase diagram were checked for mixtures of types (1-sphere + 3-sphere ring) and (1-sphere + 3-sphere chain).

Calculations at two reduced temperatures ( $T_r = T/T_{c1} = 0.6, 0.7$ ) were performed and the results are shown in Figure 6a. Clearly, as the temperature increases, the difference in behavior becomes more pronounced, with the mixture containing the cyclic component always showing more positive deviations from Raoult's law. Again, this is the experimentally observed behavior for both the (xenon + propane), (xenon + cyclopropane)

(pane) (Figure 6b) and the (xenon + butane), (xenon + cyclobutane) pairs.

The sphere size of component 2 (in both its linear and cyclic forms) was also changed relative to the size of sphere 1. Bigger and smaller sizes were tested, with the following ratios:  $\sigma_{22}/\sigma_{11} = 0.95, 0.97, 1.00, 1.15, 1.20$ . The results are plotted in Figure 7. As the size ratio departs from unity, more positive deviations from Raoult's law are observed in all cases. When the diameter of sphere 2 is smaller than that of sphere 1, the deviations from Raoult's law for the mixture with the cyclic component become increasingly more positive than those for the mixture with the linear component. However, when the diameter of sphere 2 is bigger than that of sphere 1, an inversion occurs at around  $\sigma_{22}/\sigma_{11} = 1.15$ , after which the deviations from Raoult's law for the mixture with the linear component become more positive. Unfortunately, there are no experimental data to validate this prediction. Suitable systems would be (krypton + propane) and (krypton + cyclopropane), since the diameter ratio for the pair xenon/krypton is about 1.20.

Finally, the effect of the ratio of the mean-field attraction parameters per segment for the two components was investigated. The following values were considered:  $a_{22}/a_{11} = 0.6, 0.8, 0.9, 1.0, 1.2, 1.3$ . The results of the theoretical calculations—Figure 8—predict that, as the interactions between molecules 2 become stronger ( $a_{22}/a_{11} > 1$ ), the deviations from Raoult's law become increasingly more positive for the mixtures with the cyclic component in comparison with those for the mixture with the linear component. On the other hand, if the 2–2 interactions become weaker than the 1–1 interactions ( $a_{22}/a_{11} < 1$ ), an inversion occurs, and it is now the mixture with the linear component that exhibits more positive deviations from Raoult's law.

For lack of available data, these predictions cannot be tested again. However, since there is an obvious relation between polarity and the attractive mean-field parameter, the comparison between the experimental results for mixtures involving either polar, linear, or cyclic molecules should provide, at least, a qualitative test of the theoretical predictions. A good example is that of the previously studied (xenon + dimethyl ether)<sup>6</sup> and (xenon + ethylene oxide)<sup>3</sup> systems, with their nonpolar analogues (xenon + propane) and (xenon + cyclopropane). The experimental results show that a mixture involving a polar cycle, e.g. (xenon + ethylene oxide), exhibits much larger positive deviations from Raoult's law than the corresponding mixture with either a nonpolar cycle (xenon + cyclopropane) or a polar linear molecule (xenon + dimethyl ether) (Figure 9). This is, indeed, what the theory predicts.

**Acknowledgment.** This work has been financially supported by Programa Plurianual. One of us (E.J.M.F.) gratefully acknowledges a grant through the European Scientific Exchange Program between the Lisbon Academy of Sciences (ACL) and the Royal Society. Another of us (L.M.B.D.) would like to thank the Evergreen Foundation for support.

## References and Notes

- (1) Calado, J. C. G.; Filipe, E. J. M.; Lopes, J. N. C.; Lúcio, J. M. R.; Martins, J. F.; Martins, L. F. G. *J. Phys. Chem. B* **1997**, 101, 7135.
- (2) Calado, J. C. G.; Filipe, E. J. M.; Martins, L. F. G. Manuscript in preparation.
- (3) Calado, J. C. G.; Deiters, U.; Filipe, E. J. M. *J. Chem. Thermodyn.* **1996**, 28, 201.
- (4) Calado, J. C. G.; Filipe, E. J. M.; Gomes de Azevedo, E. J. S.; Martins, L. F. G.; Soares, V. A. M. Submitted to *J. Phys. Chem.*
- (5) Calado, J. C. G.; Filipe, E. J. M.; Martins, L. F. G. Submitted to *J. Phys. Chem.*
- (6) Calado, J. C. G.; Rebelo, L. P. N.; Streett, W. B.; Zollweg, J. A. *J. Chem. Thermodyn.* **1986**, 18, 931.

- (7) Sear, R. P.; Jackson, G. *Mol. Phys.* **1994**, *81*, 801.
- (8) Galindo, A.; Whitehead, P. J.; Jackson, G.; Burgess, A. N. *J. Phys. Chem.* **1996**, *100*, 6781.
- (9) Chapman, W. G.; Gubbins, K. E.; Jackson, G.; Radosz, M. *Ind. Eng. Chem. Res.* **1990**, *29*, 1709.
- (10) Hansen, J.-P.; McDonald, I. R. *Theory of Simple Liquids*, 2nd ed.; Academic Press: London, 1986.
- (11) Boublik, T. *J. Chem. Phys.* **1970**, *53*, 471.
- (12) Mansoori, G. A.; Carnahan, N. F.; Starling, K. E.; Leland, T. W. *J. Chem. Phys.* **1971**, *54*, 1523.
- (13) Chapman, W. G.; Jackson, G.; Gubbins, K. E. *Mol. Phys.* **1988**, *65*, 1057.
- (14) Green, D. G.; Jackson, G. *J. Chem. Soc., Faraday Trans.* **1992**, *88*, 1395.
- (15) Jackson, G.; Gubbins, K. E. *Pure Appl. Chem.* **1989**, *61*, 1021.
- (16) Martin, M. L.; Youings, J. *Aust. J. Chem.* **1980**, *33*, 2133.
- (17) Gómez-Ibanez, J.; Shieh, J. J. C.; Thorsteinson, E. M. *J. Phys. Chem.* **1966**, *70*, 1998.
- (18) Gómez-Ibanez, J.; Shieh, J. J. C. *J. Phys. Chem.* **1965**, *69*, 1660.
- (19) Mairs, T. E.; Swinton, F. L. *J. Chem. Thermodyn.* **1980**, *12*, 575.
- (20) Weiguo, S.; Qin, A. X.; McElroy, P. J.; Williamson, A. G. *J. Chem. Thermodyn.* **1990**, *22*, 905.
- (21) Marsh, K. N.; Ott, J. B.; Costigan, M. J. *J. Chem. Thermodyn.* **1980**, *12*, 343.
- (22) Marsh, K. N.; Ott, J. B.; Richards, A. E. *J. Chem. Thermodyn.* **1980**, *12*, 343.
- (23) Marsh, K. N.; Ott, J. B.; Stokes, R. H. *J. Chem. Thermodyn.* **1981**, *13*, 371.